Secondary self-assembly of supramolecular nanotubes into tubisomes and their activity on cells

Johannes C. Brendel,[a,‡] Joaquin Sanchis, [b‡] Sylvain Catrouillet,[a] Ewa Czuba,[b] Moore Z. Chen [b], Benjamin M. Long,[c] Cameron Nowell,[b] Angus Johnston,[b] Katrina A. Jolliffe,[c]* and Sébastien Perrier[a,b,d]*

Abstract: The properties and structures of viruses are directly related to the three dimensional structure of their capsid proteins, which arises from a combination of hydrophobic and supramolecular interactions, such as hydrogen bonds. The design of synthetic materials demonstrating similar synergistic interactions still remains a challenge. Here, we report the synthesis of a polymer/cyclic peptide conjugate, which combines the capability to form supramolecular nanotubes via hydrogen bonds with the properties of an amphiphilic block copolymer. The analysis of aqueous solutions by scattering and imaging techniques revealed a barrel shaped alignment of single peptide nanotubes into a large tubisome (length: 250 nm) with a hydrophobic core (diameter: 16 nm) and a hydrophilic shell. These systems, which have a structure that is similar to a virus, were tested *in-vitro* to elucidate their activity on cells. Remarkably, the rigid tubisomes demonstrated the ability to perforate the lysosomal membrane in cells and release a small molecule into the cytosol.

The self-assembly and folding of small molecules or proteins, respectively, in larger macromolecules and nanostructured materials governs the formation of most natural biomacromolecules and biomaterials for instance the secondary, tertiary and quaternary structure of proteins and viruses, and the self-assembly of lipids into the lipid bilayer that forms the membrane of cells.[1] Although most synthetic systems rely on a single type of interactions, e.g. amphiphilic assemblies,[2] H-bonds,[3] electrostatic interactions,[4] π-stacking,[5] etc. examples of materials that combine two or more of these interactions to influence the overall structure of the assembly are in contrast very scarce.[6] The complementarity of hydrophobic interactions (from amphiphilic systems) and further non-covalent interactions such as hydrogen bonds or π-stacking in small molecules is particularly interesting as it has led to complex nanostructured materials exhibiting exciting properties.[7] For instance, Stupp and coworkers have developed peptide amphiphiles, which lead to nanofibers and have found applications in the biomedical field, and Aida and coworkers have formed nanotubes form amphiphilic hexabenzocoronene core substituted by phenyl triethylene glycol and dodecyl chains.[8] The translation of the synergy between hydrophobic interactions and supramolecular bonds to larger macromolecules is much more challenging, due to the polydisperse nature of synthetic polymeric chains.[9] Until now, focus has been on the manipulation of polymer chain properties, or the design of quasi block copolymers.[10] Interestingly, most examples to date have focused on the development of materials showing novel macroscopic properties, rather than the engineering of nano-objects with intrinsic features such as those found in nature. Indeed, the precise nanostructure of viruses is based on the self-organisation of proteins based on hydrogen bonding and hydrophilic / hydrophobic interactions of amino acid sequences.[11] This complementary in amphiphilic and supramolecular interactions has been harnessed by nature to develop complex functionalities, found for instance in the delivery mechanisms employed by viruses.[12] It is therefore surprising that the combination of long ranging supramolecular and amphiphilic block copolymer self-assembly remains almost unexplored, despite the immense potential to control structures on size scales ranging from few nanometers up to micrometers.[13]

A robust supramolecular interaction is a key element to engineer a macromolecule that synergistically combines both hydrophobic and supramolecular bonds. Among the myriad of supramolecular motives available, cyclic peptides (CP) consisting of alternating L- and D-amino acids are very promising candidates, as they can stack through anti-parallel ß-sheet interactions and form nanotubes with lengths of several micrometres.[14] Ghadiri, Granja et al. thoroughly studied these systems and found potential applications as transmembrane channels or antibacterial agent.[15] Moreover, the planar structure allows the selective modification of the amino acid residues, which are projected perpendicular to the tubular structure. The attachment of polymer chains to these residues increases solubility in various solvents,[16] and results in rigid, tubular supramolecular polymer brushes, which can be used to form pores in lipid bilayers or as efficient drug carrier systems.[17]

We envisaged the development of cyclic peptide/polymer conjugates which combine the character of amphiphilic block copolymers with the strong interaction between the peptides in the center (Figure 1) in contrast to the previously reported purely hydrophobic Janus conjugate.[17a] The hydrophilic part consists of poly(ethylene glycol) (PEG) chains grafted to a polyacrylate backbone (poly(PEG acrylate), pPEGA), while the hydrophobic part is made of poly(*n*-butyl acrylate) (pBA). Attaching these polymers selectively to opposite sides of the cyclic peptide leads to an amphiphilic, asymmetric polymer/CP conjugate, which demonstrates an unprecedented self-assembly in aqueous solution, driven by both the H-bond assembly of the cyclic peptide to form Janus amphiphilc nanotubes, which hydrophobic interactions in aqueous solution drive assembly into suprastructures, mimicking the secondary and tertiary/quaternary structure found in proteins. In addition, their hydrophobic cavity for cargo encapsulation, their asymmetric aspect ratio and their

[a] Dr JC Brendel, Dr S Catrouillet, Professor S Perrier
Department of Chemistry, University of Warwick, Gibbet Hill Road, Coventry CV4 7AL, UK
E-mail: s.perrier@warwick.ac.uk
[b] Dr J Sanchis, Dr E Czuba, Dr MZ Chen, Dr A Johnston
Faculty of Pharmacy and Pharmaceutical Sciences, Monash University, 381 Royal Parade, Parkville, VIC 3052, Australia
[c] Dr BM Long, Professor KA Jolliffe
The University of Sydney, School of Chemistry, Building F11, Sydney NSW 2006, Australia
[d] Professor S Perrier
Warwick Medical School, The University of Warwick, Coventry CV4 7AL, UK
‡ These authors contributed equally.

Supporting information for this article is given via a link at the end of the document.

ability to disassemble into individual conjugates to facilitate their elimination are reminiscent of virus structures and functionalities.[11]

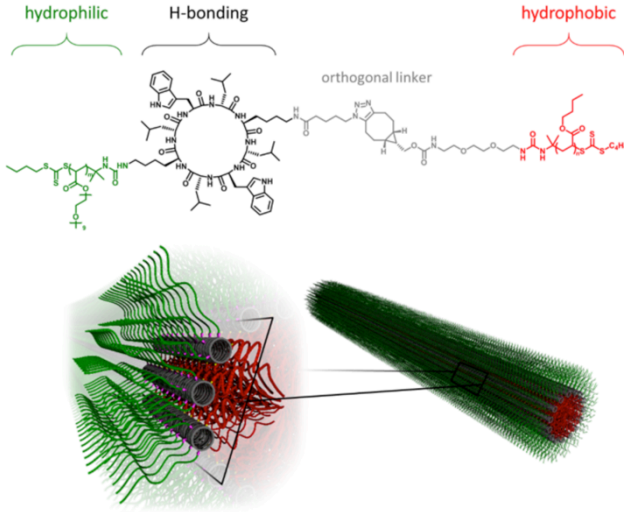

Figure 1. Structure of the amphiphilic cyclic peptide/polymer conjugate pBA-CP-pPEGA (top) and the schematic self-assembly into tubisomes (bottom).

To design our systems, we chose a convergent synthetic route, where the peptide is obtained by solid phase synthesis, and the polymeric chains of well-controlled molecular weight are synthesised by reversible addition−fragmentation chain-transfer (RAFT) polymerization. Following a protocol we reported recently, polymers of narrow molecular weight distribution (pBA and pPEGA) with highly reactive isocyanate end-groups were obtained (details on synthesis and characterisation are given in the SI).[18] Without need for post-polymerization purification, pPEGA functionalised with an isocyanate end group is added to the lysine residue on the peptide. The pBA precursor, also bearing an isocyanate chain-end group was first modified with a commercially available amine functional strained alkyne through simple mixing, followed by addition to the azide moiety introduced on the peptide, by a catalyst free strain promoted azide-alkyne cycloaddition (SPAAC).[19] The true orthogonality of both “click” reaction (isocyanate-amine addition and SPAAC) is the key advantage of our synthesis strategy, which enables the versatile preparation of amphiphilic conjugates in one sequential reaction procedure without the need for purification of any polymer intermediate (full characterization data are given in SI).

To elucidate the mechanism of self-assembly, we examined the structures using neutron and light scattering and microscopy techniques. Small angle neutron scattering (SANS) and static light scattering (SLS) revealed a distinct difference between the CP conjugates (Figure 2a, left) and the respective block copolymers (Figure 2a, right). Although the composition of the polymer blocks in both materials is similar, the block copolymer pBA_{27}-*b*-$pPEGA_{45}$ forms hairy spherical polymer micelles, as expected, with a core diameter of 5.6 nm, whereas the scattering data of the conjugates suggests a hairy rod like cylindrical structure. A clear indication for this rod-like structure is the observed q^{-1}-dependence of the scattering intensity at low q (10^{-3} – 10^{-2}). Furthermore, the q^{-2} dependence of the scattered intensity at high q (10^{-1} – 1) is characteristic of flexible polymeric chains, characteristic of a hairy objects. Therefore, a form factor of hairy rod-like micelle was used to fit the data.[20] The hairy rod-like micelles have an average length of 260 nm, but are polydisperse, as indicated by the poor fit of the sharp peaks of the model. Similar rod-like structures have been previously observed for symmetric cyclic peptide/polymer conjugates.[16a] However, in contrast to previously reported systems, the scattering data obtained here suggests a core-shell structure with and core diameter of 15 nm, which is exceeding by far the size of a single nanotube (an eight amino acid CP has an internal diameter of 0.75 nm).[21] Such a large diameter can be explained by a barrel shaped arrangement of several single nanotubes, driven by hydrophobic interaction of the Janus corona, leading to the formation of a supra-structure that we coined tubisome (based on the terms liposome and polymersome). Similar to the block copolymer micelle, the core consists of the hydrophobic pBA, while the hydrophobic pPEGA forms the hairy shell. Instead of the energetically favoured spherical structure, the strong supramolecular interaction of the cyclic peptides forces the material into an elongated, rigid shape. Atomic force microscopy (Figure 2b) confirm this observation, by showing rod like shapes with dimensions in good agreement with the scattering data, average length of 235 ± 64 nm, width of 77 ± 8 nm and maximum height of 8 ± 1 nm (further AFM images for the calculations are given in Figure SI 8). The strong deviation in width and height from the diameter determined by SANS is due to the tubisomes flattening upon drying on the surface. The low glass transition temperature of the pBA renders core more liquid-like, which cannot maintain the initial barrel shape and results in a collapse of the core in this dried state. The calculated cross-section, however, still matches with the expected structure from SANS. The ß-sheet structure was further confirmed by FTIR with the presence of the characteristic bands at 1541 and 1624 cm^{-1} for the amide II and amide I region, respectively (See figure SI 9).[22]

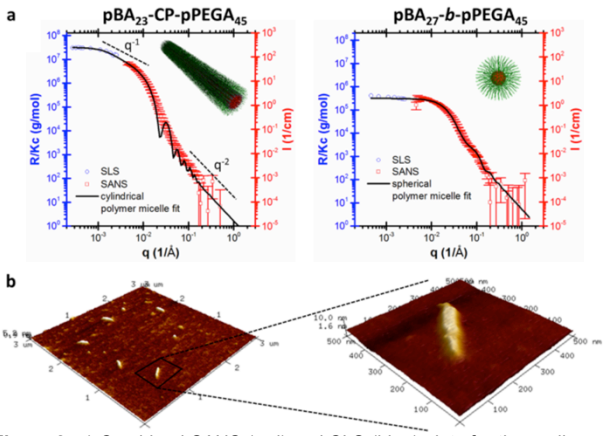

Figure 2. a) Combined SANS (red) and SLS (blue) plots for the cyclic-peptide conjugate pBA_{23}-CP-$pPEGA_{45}$ (left) and the homologous block copolymer pBA_{27}-*b*-$pPEGA_{45}$ (right). The scattering profiles were best fit with a cylindrical and spherical polymer micelle fit, respectively (black line). Details of the fit are given in SI. The insets show a schematic model for the individual fits and the dashed lines are guides for the eye to highlight the characteristic scattering profiles in the data. b) Atomic force microscopy (AFM) images (3D reconstruction of height image) of drop cast dispersions of pBA_{23}-CP-$pPEGA_{45}$ on a silicon wafer at low (left) and higher (right) magnification.

We have previously shown that hydrophobic nanotubes formed from the assembly of CP polymer conjugates can fuse with a lipid bilayer to form a channel that causes the release of a dye from an artificial vesicle.[17a] We performed a similar assay with our amphiphilic tubisomes, which also comprise the lipophilic pBA domain, on calcein entrapped 1-palmitoyl-2-oleoyl-sn-glycero-3-phosphocholine (POPC) large unilaminar vesicles (LUV) to assess if these amphiphilic structures can also interact with lipid bilayers (See SI 10). We observe a release of the dye from the LUVs, thus suggesting that the tubisomes do perforate the lipid bilayers. As observed previously, the dye

leakage is not related to a burst of the LUVs, but a diffusion through macropores in the bilayer, which impedes a 100% release.[17a] Based on these successful results on a model membrane, we were interested in establishing the effect of the tubisomes on natural lipid bilayers of cell membranes (HEK293 human embryonic kidney cell line), as a mimic of the pore formation mechanism employed by some non-enveloped viruses. Cell viability tests (MTT) showed that the tubisomes have no effect on HEK293 cell growth for concentrations up to 250 µg/ml, suggesting they are nontoxic at concentrations relevant for bioapplications (Figure 3a). The histogram-deconvolution analysis obtained with the HD-flow algorithm revealed that tubisomes fluorescently labelled with AlexaFluor488 (AF488) were associated with less than 9% of the total HEK293 cells after 3 hrs incubation at 4ºC (Figure 3b, SI 11 and SI 12). On the other hand, labelled tubisomes were found associated to 99% of the cells when they were incubated at 37ºC for a similar period of time. The concentration of tubisomes associated with these cells was increased upon the incubation-time. Confocal fluorescence microscopy shows that the AF488-labelled tubisomes can be found confined in cell compartments after incubation (Figure 3d). This result suggests that either the tubisomes are endocytosed in the fluid phase, or they fuse with the plasma membrane at 37ºC and are endocytosed as part of normal membrane turnover. Irrespective of the initial step in their mechanism of internalization, the tubisomes are observed to be localized after 24h in lysosomes, marked (red) with LAMP1-RFP (Figure 3d, image with increased contrast: Figure SI 13). Remarkably, around 70% of the marked lysosomes contain tubisomes (Figure SI 14).

In order to further ascertain the colocalisation, several pH-dependent fluorescent probes (pHrodo red dextran 10,000 Mw, pHrodo green dextran 10,000 Mw, and LysoSensor Green DND-189) were co-administered with pBA_{23}-CP-$pPEGA_{45}$ in HEK293. Cells incubated only with pHrodo red or green dextran showed a strong fluorescent signal, as the signal from pHrodo is enhanced by the acidic environment of the lysosome (~ pH 5.5). To our surprise, pre-treating samples for 16 h with both labelled (Figure 3e-g and SI 16e-g) and unlabelled (Figure SI 15, SI 16a-d and SI 17) pBA_{23}-CP-$pPEGA_{45}$ let to almost complete loss of fluorescence of pHrodo (Figure 3g, SI 15c, SI 16c-g and SI 17c). A control experiment performed under equivalent conditions with pBA_{27}-*b*-$pPEGA_{45}$ confirmed the effect was due to the conjugate structure (Figure SI 15b, SI 16b and SI 17b). Similar results were obtained when LysoSensor green DND-189 was used instead of pHrodo dye (Figure SI 18).

This loss of fluorescence suggests the lysosomes are made porous in presence of the tubisomes and promote H^+ exchange, thus leading to increase in pH and quenching of the fluorescent probes. Quantification of this effect by flow cytometry revealed 40% of quenching in the pHrodo fluorescence (red) upon 16h co-incubation with the unlabeled tubisomes (Figure 3c). To ensure the quenching is not related to an interaction of the pHrodo with the tubisomes control experiments were performed and no quenching of fluorescence was observed (Figure SI 19). We hypothesised that once encapsulated within the lysosomes, the tubisomes insert themselves in the lipid bilayer of the lysososme, possibly by presenting their hydrophobic shell, and either disrupt the membrane or create a hydrophilic channel that allows free transfer between the inside of the lysosome and the cytosol, thus leading to pH equilibration (around 7.4). However, whether the mode of action is membrane disruption or channel formation, and in the latter case, whether the effect is due to a central tubisome hydrophilic core formed by the PEGA arms or due to the channel from individual CP rings cannot be determined by the tracker experiments.

In order to characterise the properties of the tubisomes further, we performed a calcein escape assay.[23] HEK293 (pre-treated for 16 h with either pBA_{23}-CP-$pPEGA_{45}$ or pBA_{27}-*b*-$pPEGA_{45}$) were exposed for 30 min to a calcein solution in PBS. Calcein is known to internalize rapidly and can be found in lysosomes, although its fluorescence is quenched due to its high concentrations in this compartment. Around 3% (28 cells with escape out of 900) of the healthy cells treated with the tubisome shown escape of calcein (Figure 4f and Figure SI 20e for full 5x5 montage). These numbers are in agreement with the observed behaviour of the tubisomes in similar experiments with artificial membranes (LUV assay, Figure SI 10).

Further control experiments using analogous block copolymer micelles (pBA_{27}-*b*-$pPEGA_{45}$), demonstrate the importance of the tubisomes structure, as only negligible amounts of calcein release was observed for the block copolymers (3 escapes in 991 cells, 0.3%) or for the HEK control experiment (1 escape in 1134 cells, 0.08%), Figure 4e, 4d and SI 20c and SI 20a, respectively. Although it is not possible to conclude on the mode of action of the tubisomes for lysosomal escape, these nanostructures clearly affect the lysosome structure, either through membrane disruption, or by inserting themselves in the lipid bilayer and forming transmembrane channels, similarly to non-enveloped pore-forming virus.[24] Interestingly, although the tubisomes are found in the majority of the lysosomes (Figure 3c) and quenches the pHrodo-dex fluorescence (Figure 3g), only 3% of the cells display calcein release. A possible explanation is that the hydrophilic channels created by the PEG layer are sterically hindered by the PEG brushes, which would affect diffusion of calcein but not proton exchange, which can also occur through the cyclic peptide internal channels.

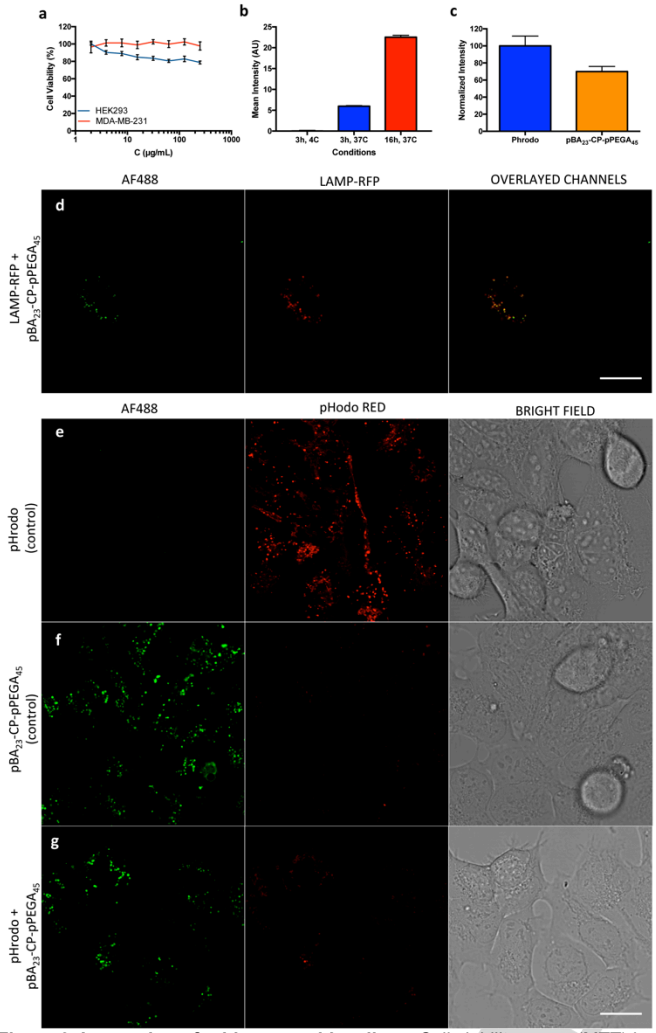

Figure 3. Interaction of tubisomes with cells. a. Cell viability assay (MTT) in two different cell lines HEK293 (Kidney) and MDA-MB-231 MH (triple negative highly metastatic breast cancer) after 72h of exposure to pBA_{23}-CP-$pPEGA_{45}$. **b.** Association profile of A488 labelled pBA_{23}-CP-$pPEGA_{45}$ in HEK293 followed by flow cytometry at different temperatures and times. **c.** Quantification by flow cytometry of the quenching of the pHrodo-dextrane fluorescence (red) in presence of pBA_{23}-CP-$pPEGA_{45}$. **d.** Lysosomal association assay. Lysosomes are marked with CellLight LAMP1-RFP (red) and pBA_{23}-CP-$pPEGA_{45}$ is labelled with Alexa-488 dye (green). **e-g** permeabilization of the lysosomal membrane estimated by the quenching of the fluorescence followed by confocal microscopy in pHrodo-dextrane probe (red). pBA_{23}-CP-$pPEGA_{45}$ is labelled with Alexa 488 (green). Scale bar indicates 20 µm.

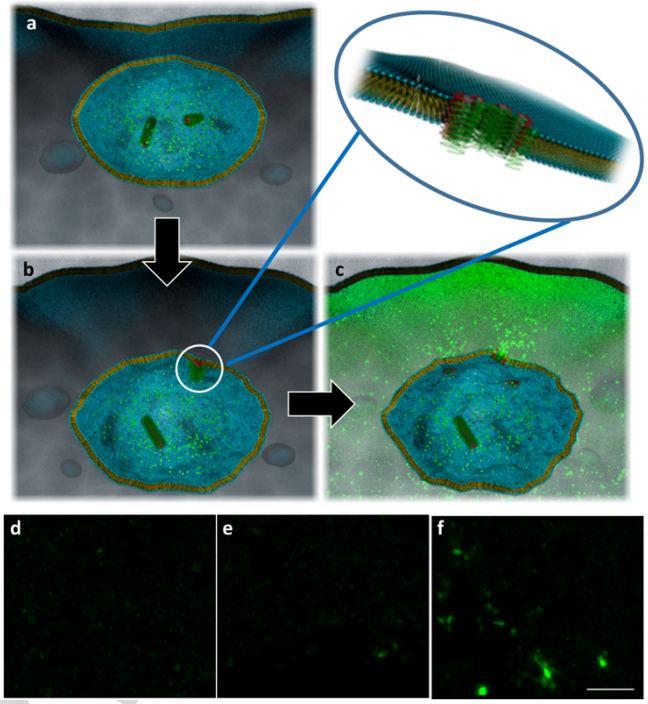

Figure 4. Calcein release from the lysosome. **a-c.** Artistic representation of the dye (green dots) release into the cytosol caused by the tubisomes **a.** early endosome: tubisomes are internalized by endocytosis **b.** late endosome/lysosome: time and confinement favour the association of the tubisome with endosomal membrane and transmembrane pore formation or membrane disruption (magnified) **c.** dye release from lysosome (the fluorescence intensity of the dye increases when released). **d.** Escapes from HEK293 cells doped with calcein for 30 min, from the same system pretreated for 16h with pBA_{27}-b-$pPEGA_{45}$ (**e**) or with pBA_{23}-CP-$pPEGA_{45}$ (**f**). Scale bar indicates 200 um.

In conclusion, we have engineered supramolecular nanostructures based on the self-assembly of amphiphilic Janus nanotubes into tubisomes, which present a hydrophobic internal channel and a hydrophilic shell. These tubisomes were shown to be non-toxic, internalised by endocytosis, and have the property to insert within the lipid bilayer of lysosomes in contrast to the equivalent block copolymer. Although only 3% of the cells were affected, our studies prove that they are able to disrupt the membrane or possibly create transmembrane channels that facilitate the escape of molecules with similar sizes to conventional drugs. The materials we report here are unique and their lysosomal escape properties highlights their potential as drug delivery vectors, which functionality can easily be controlled and tuned.

Experimental Section

See Supporting Information.

Acknowledgements

The Royal Society Wolfson Merit Award (WM130055; SP), the Monash-Warwick Alliance (JB; JSM; SP) and the European Research Council (TUSUPO 647106; SP) are acknowledged for financial support. Further, JB thanks the German Science Foundation (DFG) for granting a full postdoctoral fellowship (BR 4905/1-1).

Keywords: cyclic peptides • nanotubes • supramolecular assemblies • lysosomal escape

[1] a) M. J. E. Sternberg, J. M. Thornton, *Nature* **1978**, *271*, 15-20; b) M. J. Webber, E. A. Appel, E. W. Meijer, R. Langer, *Nat. Mater.* **2016**, *15*, 13-26; c) G. van Meer, D. R. Voelker, G. W. Feigenson, *Nat. Rev. Mol. Cell Biol.* **2008**, *9*, 112-124; d) J. N. Israelachvili, in *Intermolecular and Surface Forces (Third Edition)*, Academic Press, San Diego, **2011**, pp. 577-616.

[2] a) A. Blanazs, S. P. Armes, A. J. Ryan, *Macromol. Rapid Commun.* **2009**, *30*, 267-277; b) A. H. Groschel, A. H. E. Muller, *Nanoscale* **2015**, *7*, 11841-11876.

[3] W. Binder, in *Adv. Polym. Sci., Vol. 207*, Springer, Heidelberg, **2007**.

[4] D. V. Pergushov, A. H. E. Muller, F. H. Schacher, *Chem. Soc. Rev.* **2012**, *41*, 6888-6901.

[5] a) F. Würthner, C. R. Saha-Möller, B. Fimmel, S. Ogi, P. Leowanawat, D. Schmidt, *Chem. Rev.* **2016**, *116*, 962-1052; b) W. Wolfgang, W. Marius, S. Vladimir, O. Soichiro, W. Frank, *Angew. Chem. Int. Ed.* **2017**, *56*, 16008-16012.

[6] T. Aida, E. W. Meijer, S. I. Stupp, *Science* **2012**, *335*, 813-817.

[7] a) J. Israelachvili, R. Pashley, *Nature* **1982**, *300*, 341-342; b) T. F. A. de Greef, E. W. Meijer, *Nature* **2008**, *453*, 171-173; c) R. Milani, et al., *Chem* **2017**, *2*, 417-426; d) F. Tantakitti, et al., *Nat. Mater.* **2016**, *15*, 469-476.

[8] a) J. D. Hartgerink, E. Beniash, S. I. Stupp, *Science* **2001**, *294*, 1684-1688; b) Y. Yamamoto, et al., *Science* **2006**, *314*, 1761-1764.

[9] A.-V. Ruzette, L. Leibler, *Nat. Mater.* **2005**, *4*, 19.

[10] a) O. Ikkala, G. ten Brinke, *Science* **2002**, *295*, 2407-2409; b) R. P. Sijbesma, et al., *Science* **1997**, *278*, 1601-1604.

[11] K. Namba, G. Stubbs, *Science* **1986**, *231*, 1401-1406.

[12] M. Kielian, F. A. Rey, *Nat. Rev. Microbiol.* **2006**, *4*, 67.

[13] a) N. Chebotareva, P. H. H. Bomans, P. M. Frederik, N. A. J. M. Sommerdijk, R. P. Sijbesma, *Chem. Commun.* **2005**, 4967-4969; b) M. Muthukumar, C. K. Ober, E. L. Thomas, *Science* **1997**, *277*, 1225-1232.

[14] M. R. Ghadiri, J. R. Granja, R. A. Milligan, D. E. McRee, N. Khazanovich, *Nature* **1993**, *366*, 324-327.

[15] a) M. R. Ghadiri, J. R. Granja, L. K. Buehler, *Nature* **1994**, *369*, 301-304; b) S. Fernandez-Lopez, et al., *Nature* **2001**, *412*, 452-455.

[16] a) R. Chapman, M. Danial, M. L. Koh, K. A. Jolliffe, S. Perrier, *Chem. Soc. Rev.* **2012**, *41*, 6023-6041; b) J. Couet, J. D. Samuel, A. Kopyshev, S. Santer, M. Biesalski, *Angew. Chem. Int. Ed.* **2005**, *44*, 3297-3301; c) J. C. M. van Hest, *Polym. Rev.* **2007**, *47*, 63-92; d) H. G. Börner, *Prog. Polym. Sci.* **2009**, *34*, 811-851.

[17] a) M. Danial, C. My-Nhi Tran, P. G. Young, S. Perrier, K. A. Jolliffe, *Nat. Commun.* **2013**, *4*, 2780; b) B. M. Blunden , R. Chapman, M. Danial, H. Lu, K. A. Jolliffe, S. Perrier , M. H. Stenzel, *Chem. Eur. J.* **2014**, *20*, 12745-12749.

[18] a) G. Gody, C. Rossner, J. Moraes, P. Vana, T. Maschmeyer, S. Perrier, *J. Am. Chem. Soc.* **2012**, *134*, 12596-12603; b) S. C. Larnaudie, J. C. Brendel, K. A. Jolliffe, S. Perrier, *J. Polym. Sci., Part A: Polym. Chem.* **2016**, *54*, 1003-1011.

[19] J. Dommerholt, et al., *Angew. Chem. Int. Ed.* **2010**, *49*, 9422-9425.

[20] J. Pedersen, *J. Appl. Crystallogr.* **2000**, *33*, 637-640.

[21] M. R. Ghadiri, K. Kobayashi, J. R. Granja, R. K. Chadha, D. E. McRee, *Angew. Chem. Int. Ed.* **1995**, *34*, 93-95.

[22] R. Chapman, M. L. Koh, G. G. Warr, K. A. Jolliffe, S. Perrier, *Chem. Sci.* **2013**, *4*.

[23] Y. Hu, T. Litwin, A. R. Nagaraja, B. Kwong, J. Katz, N. Watson, D. J. Irvine, *Nano Lett.* **2007**, *7*, 3056-3064.

[24] a) E. Prchla, C. Plank, E. Wagner, D. Blaas, R. Fuchs, *J. Cell Biol.* **1995**, *131*, 111-123; b) S. Suikkanen, M. Antila, A. Jaatinen, M. Vihinen-Ranta, M. Vuento, *Virology* **2003**, *316*, 267-280; c) W. Dowling, E. Denisova, R. LaMonica, E. R. Mackow, *J. Virol.* **2000**, *74*, 6368-6376; d) M. A. Agosto, T. Ivanovic, M. L. Nibert, *Proc. Natl. Acad. Sci.* **2006**, *103*, 16496-16501.

Entry for the Table of Contents (Please choose one layout)

COMMUNICATION

Polymer/cyclic peptide conjugate form supramolecular tubisome structures with a hydrophobic core and a hydrophilic shell and demonstrate the ability to perforate the lysosomal membrane in cells to release a small molecule into the cytosol.

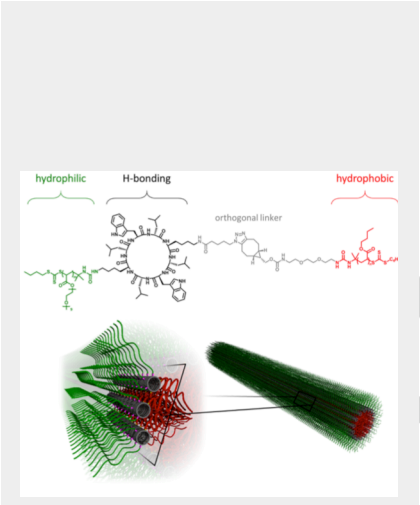

*Johannes C. Brendel,[a,‡] Joaquin Sanchis Martinez,[b‡] Sylvain Catrouillet,[a] Ewa Czuba,[b] Moore Z. Chen[b], Benjamin M. Long,[c] Cameron Nowell,[b] Angus Johnston,[b] Katrina A. Jolliffe,[c] * and Sébastien Perrier[a,b,d] **

XX - XX

Secondary self-assembly of supramolecular nanotubes into tubisomes and their activity on cells